

# Fiber-connected UWB sensor network for high-resolution localization using optical time-division multiplexing

Jianbin Fu and Shilong Pan\*

Microwave Photonic Research Laboratory, College of Electronic and Information Engineering, Nanjing University of Aeronautics and Astronautics, Nanjing 210016, China  
\*pans@ieee.org

**Abstract:** A fiber-connected ultra-wideband (UWB) sensor network for high-resolution localization which consists of a central station and several sensor nodes is proposed and demonstrated. To make the central station easily identify the received UWB pulses from different sensor nodes, optical time-division multiplexing (OTDM), realized by inserting a certain length of optical fiber between every two sensor nodes, is implemented. Due to the OTDM technology, the UWB pulses received by different sensors are mapped into different time slots, so neither parameter estimation nor clock synchronization is required in the UWB sensor node. All complex signal processing is completed in the central station, which greatly improve the localization accuracy and simplify the system. A proof-of-concept experiment for two-dimensional localization is demonstrated. Spatial resolution as high as 3.9 cm is achieved.

©2013 Optical Society of America

OCIS codes: (060.2310) Fiber optics; (060.5625) Radio frequency photonics; (280.0280) Remote sensing and sensors.

---

## References and links

1. S. Gezici, Z. Tian, G. B. Giannakis, H. Kobayashi, A. F. Molisch, H. V. Poor, and Z. Sahinoglu, "Localization via ultra-wideband radios: a look at positioning aspects for future sensor networks," *IEEE Signal Process. Mag.* **22**(4), 70–84 (2005).
2. R. Thoma, O. Hirsch, J. Sachs, and R. Zetik, "UWB sensor networks for position location and imaging of objects and environments," in the Second European Conference on Antennas and Propagation (EuCAP 2007), pp. 1–9.
3. J. Zhang, P. V. Orlik, Z. Sahinoglu, A. F. Molisch, and P. Kinney, "UWB systems for wireless sensor networks," *Proc. IEEE* **97**(2), 313–331 (2009).
4. N. Patwari, J. N. Ash, S. Kyperountas, A. O. Hero III, R. L. Moses, and N. S. Correal, "Locating the nodes: cooperative localization in wireless sensor networks," *IEEE Signal Process. Mag.* **22**(4), 54–69 (2005).
5. H. Soganci, S. Gezici, and H. Poor, "Accurate positioning in ultra-wideband systems," *IEEE Wireless Commun. Mag.* **18**(2), 19–27 (2011).
6. I. Oppermann, L. Stoica, A. Rabbachin, Z. Shelby, and J. Haapola, "UWB wireless sensor networks: UWEN-a practical example," *IEEE Commun. Mag.* **42**(12), S27–S32 (2004).
7. L. Stoica, A. Rabbachin, and I. Oppermann, "A low-complexity noncoherent IR-UWB transceiver architecture with TOA estimation," *IEEE Trans. Microw. Theory Tech.* **54**(4), 1637–1646 (2006).
8. W. M. Lovelace and J. K. Townsend, "The effects of timing jitter and tracking on the performance of impulse radio," *IEEE J. Sel. Areas Comm.* **20**(9), 1646–1651 (2002).
9. R. J. Fontana, E. Riehley, and J. Barney, "Commercialization of an ultra wideband precision asset location system," in 2003 IEEE Conference on Ultra Wideband Systems and Technologies, pp. 369–373.
10. G. Cheng, "Accurate TOA-based UWB localization system in coal mine based on WSN," *Phys. Procedia* **24**, 534–540 (2012).
11. S. L. Pan and J. P. Yao, "UWB over fiber communications: modulation and transmission," *J. Lightwave Technol.* **28**(16), 2445–2455 (2010).
12. J. C. Adams, W. Gregorowich, L. Capots, and D. Liccardo, "Ultra-wideband for navigation and communications," in *Proc. IEEE Aerospace Conf.* **2** 785–792 (2001).
13. J. Y. Lee and R. A. Scholtz, "Ranging in a dense multipath environment using an UWB radio link," *IEEE J. Sel. Areas Comm.* **20**(9), 1677–1683 (2002).
14. S. Gezici and H. V. Poor, "Position estimation via ultra-wide-band signals," *Proc. IEEE* **97**(2), 386–403 (2009).

## 1. Introduction

High-spatial-resolution localization can be realized via impulse-radio (IR) ultra-wideband (UWB) technique thanks to its advantages in terms of high time resolution, penetrating capability and possibility to construct low-cost and low-power-consumption system [1,2]. The IR-UWB localization systems are conventionally implemented based on UWB sensor networks [3,4], in which the position-related parameters such as time of arrival (TOA), angle of arrival (AOA) or received signal strength (RSS) are estimated in the UWB sensor nodes. These parameters are sent to a central station to calculate the position of the target [5]. However, each UWB sensor in this system has to process the received UWB signals independently, which increases significantly the complexity of the UWB sensors. To make the cost of the UWB sensor affordable, only very simple signal processing such as energy detection can be applied [6,7], which would sacrifice the accuracy of the system. In addition, clock synchronization between the UWB sensor nodes is complicated and usually inaccurate, which degrades again the localization accuracy [4,8]. Moreover, the UWB sensors are conventionally connected to the central station by electrical cables [9] or wireless [10], which are lossy, bandwidth-limited, and sensitive to the electromagnetic interference. On the other hand, UWB-over-fiber technique was proposed in the past decade [11], which employs optical fiber to transmit the UWB signals between the central stations and the remote antenna units with negligible distortion. The UWB-over-fiber technique also enables the centralized signal processing, which can possibly solve the problems in UWB localization systems.

In this paper, a fiber-connected UWB sensor network for high-resolution localization using optical time-division multiplexing (OTDM) is proposed and demonstrated for the first time, to the best of our knowledge. In the proposed system, the UWB sensor in the conventional UWB localization system is replaced by a UWB antenna and an electrical-to-optical conversion module (EOM). A length of single-mode fiber (SMF) is placed between every two EOMs to introduce a proper time delay for the implementation of OTDM, which maps the UWB pulses received by different UWB antennas into separated time slots. As a result, the central station can identify the received UWB pulses of different sensor nodes. The proposed system removes the complex signal processing from each UWB sensor node to the central station, making the sensor network very simple. In addition, since signal processing is concentrated in the central station which can have more resource, more complex algorithm can be adopted to achieve higher accuracy [12,13]. A proof-of-concept experiment is carried out for the two-dimensional localization of a target. Centimeter-level spatial resolution is achieved.

## 2. Principle

The schematic diagram of the proposed fiber-connected UWB sensor network is shown in Fig. 1. The system consists of a central station, a UWB source and several distributed UWB sensors in the detection zone. The central station generates a CW lightwave and processes the received optical UWB signal, and the UWB sensor node contains a UWB antenna and an EOM. A length of SMF is used to connect every two EOMs, which can also introduce a proper time delay between the two sensor nodes to implement OTDM.

An IR-UWB pulse train with a low duty cycle is generated by the UWB generator and emitted to the free space via a UWB antenna. The UWB pulses are sent to the UWB sensors via two physical paths, i.e. one goes directly from the UWB source to the UWB sensors, and the other is reflected by the target and then received by the UWB sensors. The received electrical UWB signal in each UWB sensor is converted into an optical signal at the EOM on the CW lightwave from the central station. To avoid overlapping of the UWB pulses from different UWB sensor nodes in the time domain, the lengths of the SMF between two UWB sensors are carefully chosen to map the UWB pulses received by different sensor nodes into different time slots, i.e. the period of the UWB signal train  $t_{RP}$  and the time slot of OTDM  $t_D$

should satisfy the relation  $t_{RP} > n \cdot t_D$ , where  $n$  is the number of UWB sensor nodes. The optical time-division multiplexed UWB signal is finally sent to the central station via an SMF, which is processed to extract the position information of the target.

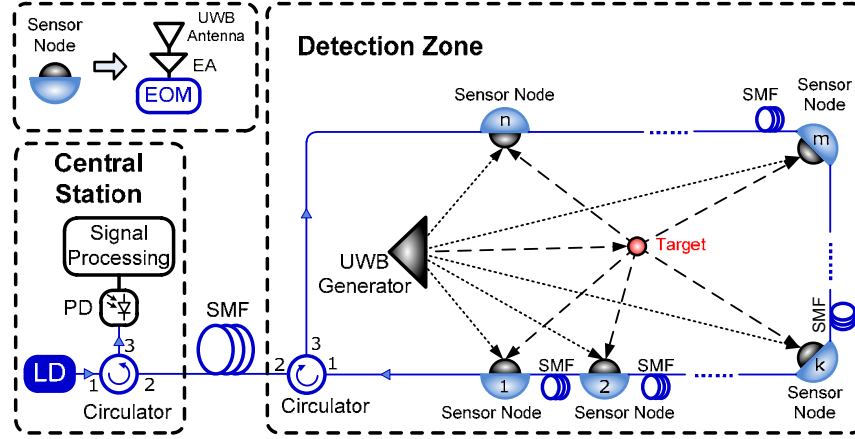


Fig. 1. Schematic diagram of the proposed fiber-connected UWB sensor network using OTDM. EA: electrical amplifier; EOM: electrical-to-optical conversion module; PD: photodetector; LD: laser diode; SMF: single-mode fiber.

In the proposed system, clock synchronization is not required because in each time slot, there are two UWB pulses, containing the information of the relative locations of the UWB source, the target and the UWB sensor. Since the locations of the UWB source and the UWB sensors are known, two UWB sensors can determine the two-dimensional location of the target in the detection zone.

The position of the target can be estimated using mapping approaches or geometric techniques [14]. In this work, a geometric method is adopted due to its high accuracy and flexibility. To simplify the mathematical manipulation, we assume a two-dimensional localization scenario using two UWB sensor nodes. Figure 2(a) shows the geometric model of the OTDM-based UWB sensor network. A typical received UWB sequence in the central station is shown in Fig. 2(b). Based on Fig. 2, the following relations can be easily obtained,

$$\begin{cases} L_{|ST|} + L_{|TA|} = L_{|SA|} + c(t_{TA} - t_A) \\ L_{|ST|} + L_{|TB|} = L_{|SB|} + c(t_{TB} - t_B) \end{cases} \quad (1)$$

where  $c$  is the velocity of light in vacuum,  $L_{|ST|}$ ,  $L_{|TA|}$ ,  $L_{|SA|}$ ,  $L_{|TB|}$ ,  $L_{|SB|}$  are the distances between the UWB source and the target, the target and node A, the UWB source and node A, the target and node B, and the UWB source and node B, respectively.  $t_A$  and  $t_B$  are the TOAs for the direct radiation from the UWB source to node A and B, and  $t_{TA}$ ,  $t_{TB}$  are the TOAs with the target reflection. Denote the coordinates of S, A, B and T by  $(x_S, y_S)$ ,  $(x_A, y_A)$ ,  $(x_B, y_B)$  and  $(x, y)$ , respectively, a set of equations for ellipses can be obtained,

$$\begin{cases} \sqrt{(x-x_S)^2 + (y-y_S)^2} + \sqrt{(x-x_A)^2 + (y-y_A)^2} = \sqrt{(x_S-x_A)^2 + (y_S-y_A)^2} + c(t_{TA}-t_A) \\ \sqrt{(x-x_S)^2 + (y-y_S)^2} + \sqrt{(x-x_B)^2 + (y-y_B)^2} = \sqrt{(x_S-x_B)^2 + (y_S-y_B)^2} + c(t_{TB}-t_B) \end{cases} \quad (2)$$

where  $(x_S, y_S)$ ,  $(x_A, y_A)$ ,  $(x_B, y_B)$  are the preset parameters because the position of the UWB source and the two nodes are already known. The parameters  $(t_{TA}-t_A)$  and  $(t_{TB}-t_B)$  can be estimated by the time difference of arrival (TDOA) from the received UWB sequence obtained in the central station, as shown in Fig. 2(b). By solving (2), the position of the target,

i.e.  $(x, y)$ , can be obtained. In practice, because the UWB source emits a pulse train with fixed period, it is important to identify which pulse in the received waveform is from the first node. This can be accomplished by allocating a bigger or smaller time slot for the first node using a longer or shorter length of fiber. It should be noted that mathematically two possible solutions can be achieved for (2), but only one solution is effective if the UWB antennas are directional. In addition, three or more UWB sensor nodes can be used to realize the three-dimensional localization or to achieve higher localization accuracy.

The proposed approach, however, is limited to the localization of single target. To identify multiple targets in the detection zone, other information such as the angle of arrival (AOA) is required. The AOA information can be collected by placing an antenna array at each sensor node, and detected at the central station using the TDOAs of the different antennas in the antenna array.

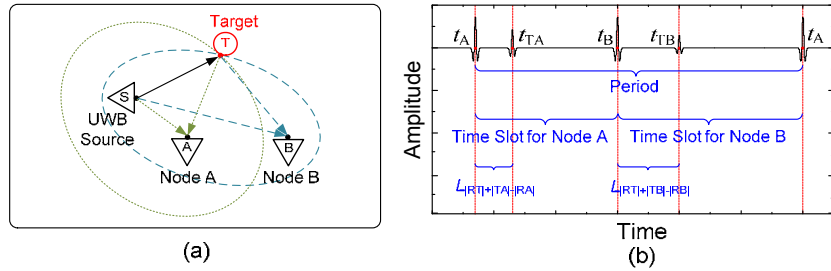


Fig. 2. Geometric method for localization in the OTDM-based UWB sensor network; (a) Geometric model of the OTDM-based UWB sensor network; (b) the simulated typical received UWB sequence.

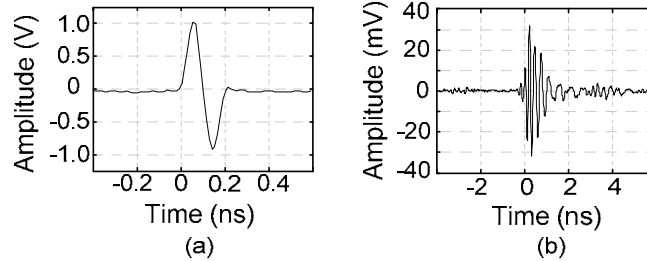


Fig. 3. The waveforms (a) generated by the UWB generator and (b) received by the UWB antenna.

### 3. Experimental validation

A proof-of-concept experiment is carried out for the two-dimensional localization of a metal target using two UWB sensor nodes. A laser source (Agilent N7714A) is used to generate the CW lightwave and two Mach-Zehnder modulators (MZMs) (Fujitsu Limited) are applied in the two UWB sensor nodes. The IR-UWB pulse train is generated by differentiating the output of a pulse pattern generator (PPG, Anritsu MP1763C). The generated UWB monocycles have a duty cycle of about 1/3200 and a period of about 256 ns. As shown in Fig. 3(a), the full width at half maximum (FWHM) of the UWB monocycle is about 160 ps. Because of the frequency response of the UWB antennas and other components, the radiated UWB pulse is shaped to have a waveform shown in Fig. 3(b). A 16-GHz real-time oscilloscope (Agilent DSO9404A) with a sampling rate of 80 GSa/s is used to record the waveform at the output of the PD in the central station. The recorded data are processed and analyzed off-line.

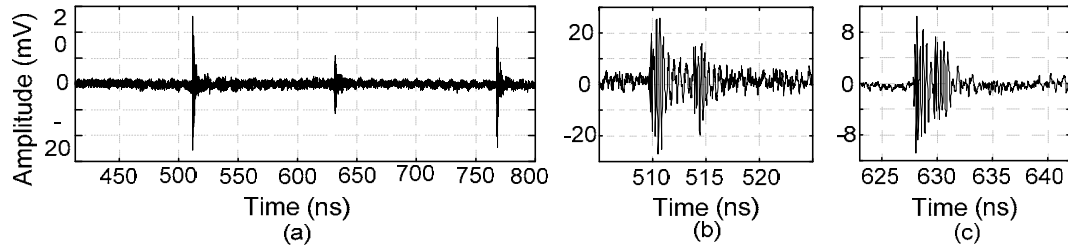


Fig. 4. (a) The waveforms recorded at the output of the PD and (b), (c) zoom-in view of the two groups of UWB waveforms.

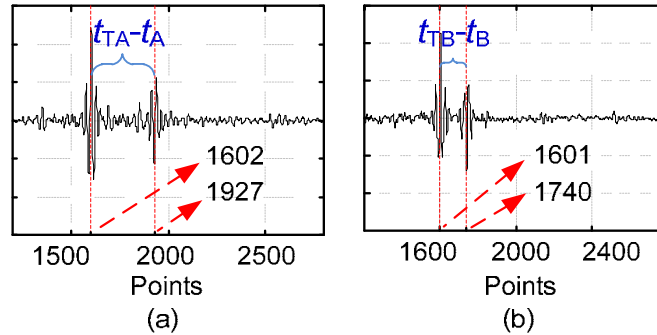


Fig. 5. Cross-correlation results for achieving TDOAs for (a) node A and (b) node B.

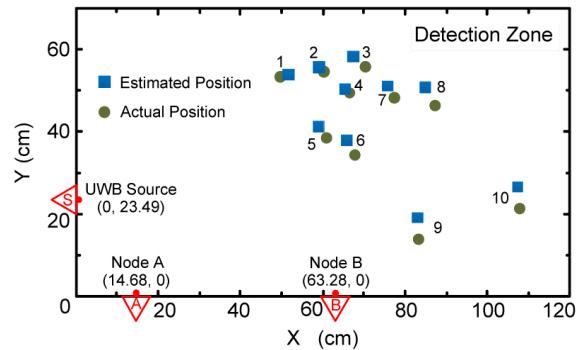


Fig. 6. The geometric locations of ten samples of the estimated positions and their corresponding actual positions.

Figure 4(a) shows the recorded waveform at the output of the PD. Two groups of UWB waveforms are presented in two time slots at  $\sim 510$  ns and  $\sim 630$  ns, respectively. The zoom-in views of the two groups of the UWB waveforms are shown in Figs. 4(b) and 4(c). To increase the accuracy of the TDOA estimation, the received UWB waveforms are cross-correlated with the waveform emitted from the UWB source, i.e. the waveform shown in Fig. 3(b). Figures 5(a) and 5(b) show the correlation results. The TDOA in the node A and B can be easily calculated:  $t_{TA}-t_A = (1927-1602) \cdot 12.5\text{ps} = 4.06$  ns,  $t_{TB}-t_B = (1740-1601) \cdot 12.5\text{ps} = 1.74$  ns, where 12.5 ps is the sampling interval of the oscilloscope. With the TDOA and considering the given positions of the UWB source, node A and node B, the position of the target can be estimated. The FWHM of the pulses after cross-correlation are about 87 ps, indicating that the theoretical localization spatial resolution is less than 2.6 cm.

**Table 1. Ten Samples of the Estimated Position of the Target**

Sample	Estimated Position	Actual Position	Error (cm)
1	(51.93, 53.81)	(50.20, 53.72)	1.73
2	(59.00, 55.64)	(60.53, 54.47)	1.93
3	(67.36, 58.03)	(70.90, 54.79)	4.80
4	(65.60, 49.96)	(67.00, 49.03)	1.68
5	(59.01, 41.27)	(60.90, 38.42)	3.42
6	(65.97, 37.78)	(67.83, 34.38)	3.88
7	(75.28, 51.72)	(77.85, 47.93)	4.58
8	(84.88, 50.80)	(87.71, 45.80)	5.75
9	(83.00, 19.18)	(83.41, 13.79)	5.41
10	(107.4, 26.57)	(108.0, 21.23)	5.37

To further investigate the accuracy of the proposed localization system, ten measurements are performed with the target placed at ten different sample locations. The estimated positions are compared with their actual positions, by which the localization errors of the system are achieved. The ten estimated positions and the actual positions are shown in Table 1 and Fig. 6. From the data in Table 1, we can calculate that the mean localization error is 3.9 cm, which is quite close to the theoretical localization spatial resolution 2.6 cm. The localization errors for Sample 8, 9 and 10 are larger than others. This may result from the directional attenuation of the directional UWB antennas. It should be noted that more complex algorithm such as averaging filtering and interpolating method [12] can be adopted to achieve even higher accuracy.

#### 4. Conclusion

A fiber-connected UWB sensor network for high-resolution localization using OTDM technology was proposed and demonstrated. Thanks to the low loss, wide bandwidth and immunity to electromagnetic interference of the optical fiber, the received UWB pulses from different sensor nodes are concentrated to the central station using a single SMF with negligible distortion. As a result, all the complex signal processing is completed in the central station, which greatly increases the localization accuracy and simplifies the configuration. The experimental results showed that the system has a spatial resolution of 3.9 cm. The proposed system may find applications in logistics, security applications, coal mine localization and military applications.

#### Acknowledgments

This work was supported in part by the National Natural Science Foundation of China (61107063), the National Basic Research Program of China (2012CB315705), the Natural Science Foundation of Jiangsu Province (BK2012031), the Fok Ying Tung Education Foundation, the Fundamental Research Funds for the Central Universities (NE2012002, NP2013101), the Project sponsored by SRF for ROCS, SEM and a Project Funded by the Priority Academic Program Development of Jiangsu Higher Education Institutions.